

UPPER ATMOSPHERIC DENSITIES DERIVED FROM STARSHINE SPACECRAFT ORBITS

R. G. Moore¹, J. Lean², J. M. Picone², S. Knowles³, A. Hedin², and J. Emmert²

1. 3855 Sierra Vista Road, Monument CO 80132

2. Naval Research Laboratory, Washington DC 20375

3. Raytheon Company, Lexington MA 02421

Abstract

Between June 1999 and January 2003 three Starshine spacecraft were launched into low-earth orbits. Their lifetimes cover an extended period near the maximum of solar cycle 23. Two additional Starshine spacecraft are ready for launch near the minimum of solar cycle 23. The Starshine missions are especially suitable for estimating average upper atmospheric densities, since the orbits are approximately circular and the spacecraft are mirrored spheres for which ballistic coefficients are essentially independent of orientation with respect to the direction of motion. We have derived total neutral atmospheric mass densities along the Starshine spacecraft trajectories using quantities from their Two-Line Element sets (TLEs). We compare these densities with corresponding determinations by a semi-empirical model of upper atmospheric neutral densities developed at the Naval Research Laboratory. This model, NRLMSIS, has been formulated for both research and operational use from a database that now includes total mass densities from satellite accelerometers and orbit determinations, more recent temperatures from incoherent scatter radar, and molecular oxygen number densities from solar UV occultation. The Starshine orbits were not included in the NRLMSIS model formulation and thus provide independent validation of the modeled variations on time scales of days to months during a period of relatively high solar activity.

The Starshine Spacecraft

The Starshine spacecraft are small spherical satellites whose mass, radii and launch dates are summarized in Table 1. Figure 1 shows the Starshine 2 spacecraft prior to launch. Its outer surface is covered with 845 aluminum mirrors, polished by 30,000 students from around the world.

Starshine Orbits and Two-Line Element Sets

The Starshine spacecraft were launched into almost circular, moderate inclination, low-earth orbits, of about one year duration. The North American Aerospace Defense Command (NORAD) tracked the orbits of each Starshine spacecraft and produced Two-Line Element sets (TLEs) that provide orbital parameters derived from General Perturbation theory. The parameters are values of the six Kozai mean elements of inclination, right ascension of the ascending node, argument of perigee, eccentricity, mean motion and mean anomaly at epoch. Additional elements relate to drag, including $\dot{n}/2$ (mean motion time derivative). The TLEs of the Starshine orbits were typically updated a few times per day, at selected times called epochs. They are available courtesy of Dr. T. Kelso at <http://www.celestrak.com>.



Figure 1. The Starshine 2 spacecraft prior to launch.

Figure 2 illustrates the variations in selected orbital parameters archived in the TLEs for each Starshine spacecraft throughout its mission.

Starshine Spacecraft	Launch	Re- entry	Initial Altitude (km)	Approximate Eccentricity	Inclination (degree)	Mass (kg)	Diameter (cm)	C _D	Inverse Ballistic Coefficient (cm ² gm ⁻¹)
1	1999 05-27	2000 02-18	385	0.001	51.6	39	48 (19")	2.1	0.097
2	2001 12-05	2002 05-01	370	0.002	51.6	38	48 (19")	2.1	0.100
3	2001 09-29	2003 01-21	475	0.001	67	90	94 (37")	2.1	0.162

Table 1. Summary of Starshine spacecraft properties.

Atmospheric Densities Derived from TLEs

The mean motion, n , of a spacecraft orbiting the Earth with velocity v , changes with time, t , because of the drag of the Earth's atmosphere. The total mass density, ρ , of the upper atmosphere along the spacecraft track relates to the change in the mean motion, dn , by

$$dn = \frac{3}{2} n^{1/3} \mu^{-2/3} B F \rho v^3 dt \quad \dots (1)$$

where $\mu = GM_E$ is the gravitational parameter, defined by G , the gravitational constant, and M_E the mass of the Earth (King-Hele, 1987). The inverse ballistic coefficient is $B = C_D A / M$ where C_D is the drag coefficient, A the cross-sectional area and M the mass of the spacecraft. Table 1 lists values of these quantities for each Starshine spacecraft.

The quantity F in Equation 1 accounts for the effect on the spacecraft of co-rotating winds in the Earth's upper atmosphere, which depends on the spacecraft's inclination, i , velocity, v , and distance, r , from the center of the Earth according to

$$F \cong \left(1 - \frac{r\omega}{v} \cos(i) \right)^2 \quad \dots (2)$$

where ω is the Earth's angular velocity.

During any single orbit the osculating mean motion varies primarily because of gravitational perturbations related to the asymmetry of the Earth's mass distribution. The effects of atmospheric drag become evident on longer time scales, over multiple orbits and relate to the mean motion through Equation 1. This means that, in general, the determination of atmospheric density, ρ , requires the integration of Equation 1 over sufficient time $\Delta t = t_2 - t_1$ to accumulate a measurable change due to drag. Using Equation 1 and

defining an effective density, ρ_E , over the time interval $t_2 - t_1$ as

$$\rho_E = \frac{\int F \rho v^3 dt}{\int F v^3 dt} \quad \dots (3)$$

the change in the mean motion, $dn = n_2 - n_1$, from t_1 to t_2 is then

$$n_2 - n_1 \cong \frac{3}{2} n_E^{1/3} \mu^{-2/3} B \rho_E \int F v^3 dt \quad \dots (4)$$

where n_E is the mean motion at the center of the time interval. The effective density is then

$$\rho_E = \frac{2}{3} (n_2 - n_1) \frac{\mu^{2/3}}{B n_E^{1/3} \int F v^3 dt} \quad \dots (5)$$

For circular orbits, the velocity and distance from the Earth's center are constant during an orbit, so that

$$\int F v^3 dt = F v^3 (t_2 - t_1) \quad \dots (6)$$

Noting that $dn/dt \sim (n_2 - n_1)/(t_2 - t_1)$ and dropping the subscript E , Equation 5 then becomes

$$\rho \cong \frac{2}{3} \frac{dn}{dt} \frac{\mu^{2/3}}{B n^{1/3} v^3 F} \quad \dots (7)$$

Figure 3 shows values of n , dn/dt , v , and F at epoch of the TLEs throughout each of the Starshine orbits. The quantities n and $dn/dt = 2(\dot{n}/2)$ are obtained from the TLEs directly. Applying the SGP4 orbital propagator to the TLEs provides estimates of the velocity, v , and the distance from the Earth's center, r , needed (together with the inclinations shown in Figure 2) to calculate F .

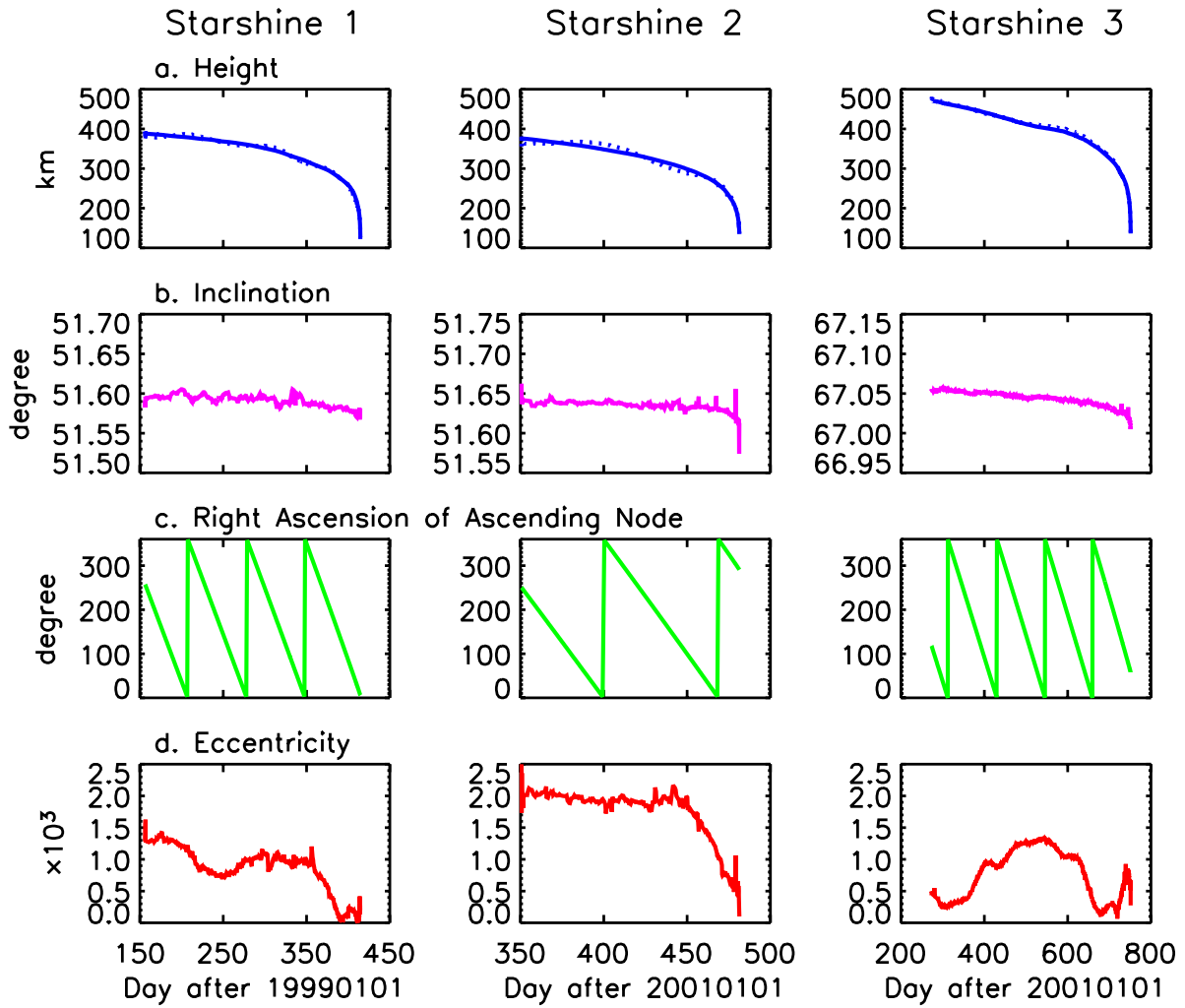


Figure 2. Shown from top to bottom are approximate altitude (semi-major axis minus Earth radius), inclination, right ascension of the ascending node and eccentricity of the Starshine spacecraft orbits throughout their missions, obtained from the TLEs.

The slight eccentricities of the Starshine orbits and the oblateness of the Earth induce small deviations of speed (shown by the dashed lines in Figure 3c) and altitude (shown by the dashed lines in Figure 2a) relative to the orbital means, that track the drift with time in the argument of perigee. The actual values of these quantities reported in the TLEs depend on the spacecraft's location in its orbit at each epoch. Figure 4 shows the variations of height above the Earth's center, r , and speed, v , within an individual orbit of each Starshine spacecraft near the beginning of its mission. The distances, velocities and wind factor corrections remain constant to better than one

percent, so that Equation 6 is approximately true and Equation 7 can be used to estimate the atmospheric density directly from the values of TLEs at epoch for each of the Starshine missions.

Evaluating Equation 7 with the quantities shown in Figure 3 produces upper atmospheric mass densities along the Starshine orbital tracks shown in Figure 5. These densities exhibit two main features. Firstly, there is an overall exponential decrease in density with increasing altitude. Secondly, prominent fluctuations are superimposed on the exponential profile. The exponential density decrease with

SSC03-V-2

altitude is similar, but less steep than that in the 1976 US Standard Atmosphere, whose total mass density is compared in Figure 6 with the profiles deduced from the Starshine orbits. The fluctuations about the mean profile, evident in the total mass densities in Figure 5, occur because of variations in the Sun's energy input to the upper atmosphere, primarily in the form of extreme ultraviolet (EUV) electromagnetic radiation.

During the Starshine missions, solar activity was at overall high levels near the peak of cycle 23, which

commenced in 1996. This is indicated by the variations in the daily sunspot numbers in Figure 7 which show that cycle 23 was not as active as the previous cycle 22, which commenced in 1986. Total EUV energy fluctuates as a result of solar activity and the Sun's rotation on its axis (once every 27-days). The EUV energy is higher during times of high solar activity (and sunspot numbers). This increased energy causes the upper atmosphere to expand, with the result that atmospheric density increases at a given altitude and spacecraft experience increased atmospheric drag.

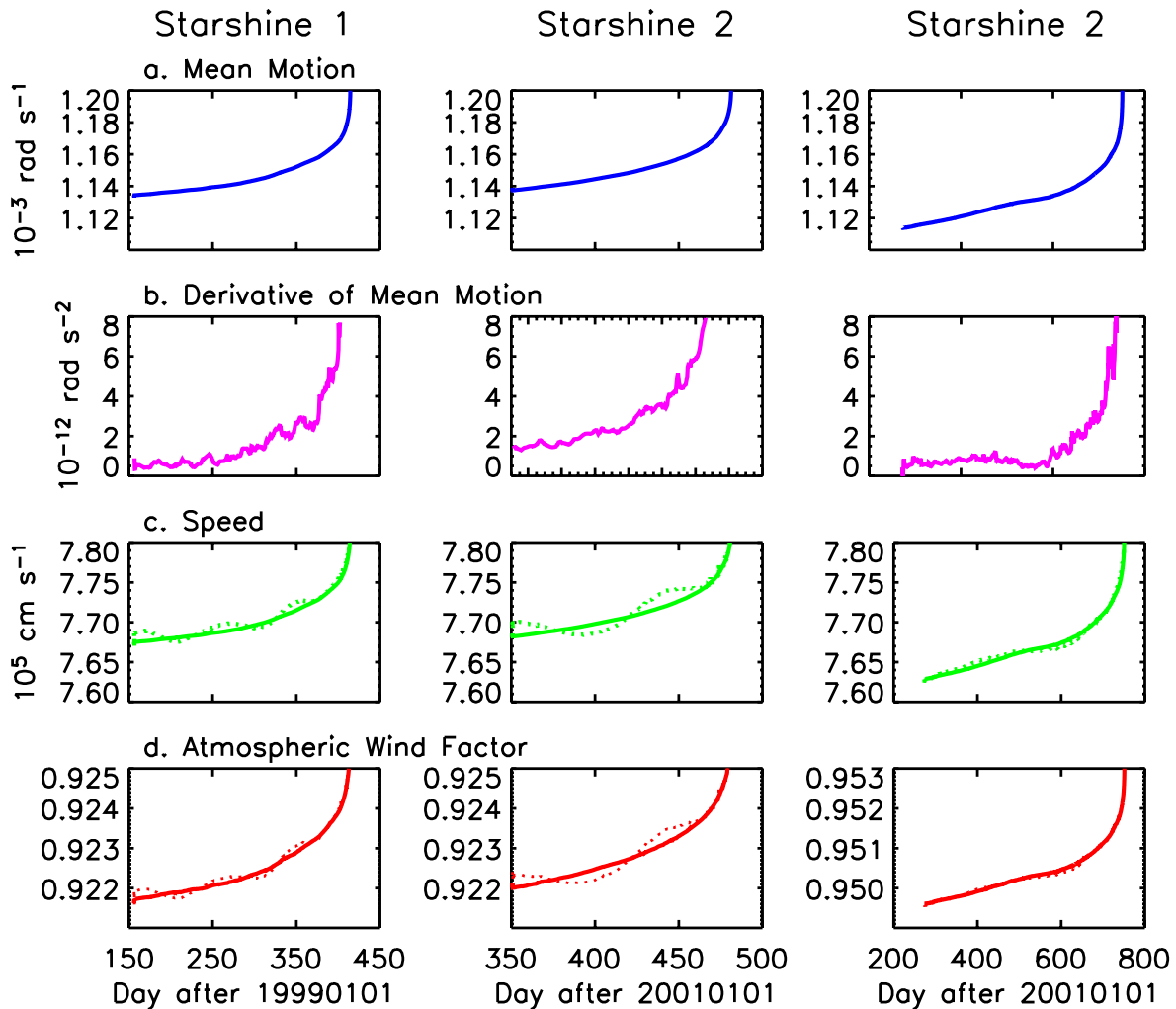


Figure 3. Shown in the four panels from top to bottom are the mean motion, its derivative, the speed and the atmospheric wind factor for each of the Starshine spacecraft, obtained from the TLEs and SGP4.

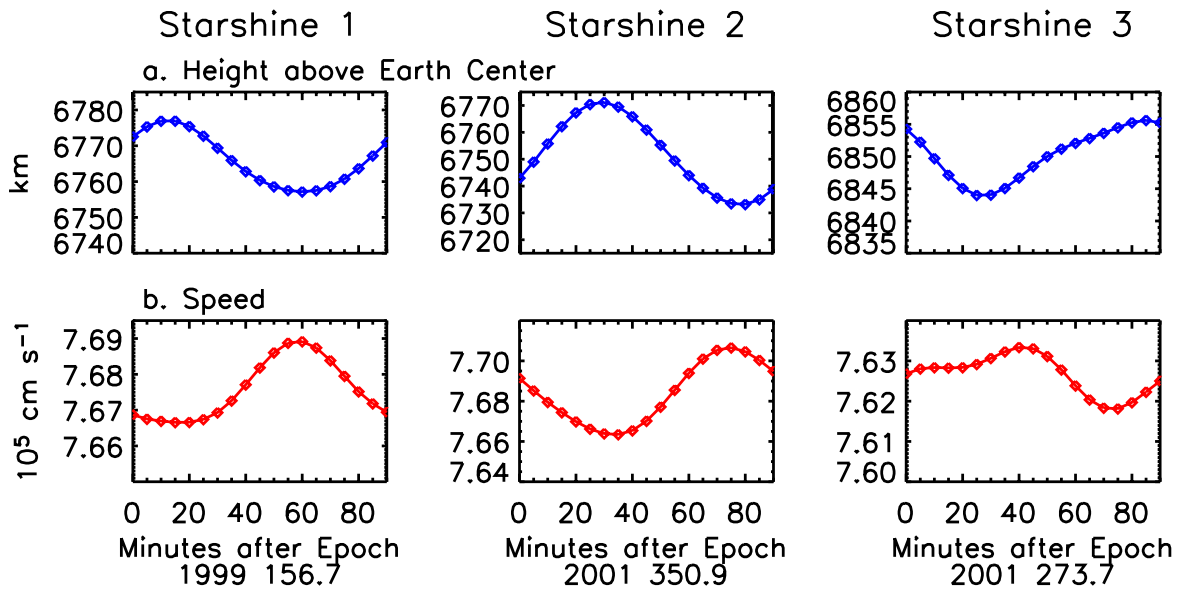


Figure 4. Shown in the top panel are the heights above the Earth's center during individual orbits of the Starshine spacecraft, and in the bottom panel the corresponding speeds, obtained by using SGP4 to propagate the orbit for 90 minutes beyond epoch.

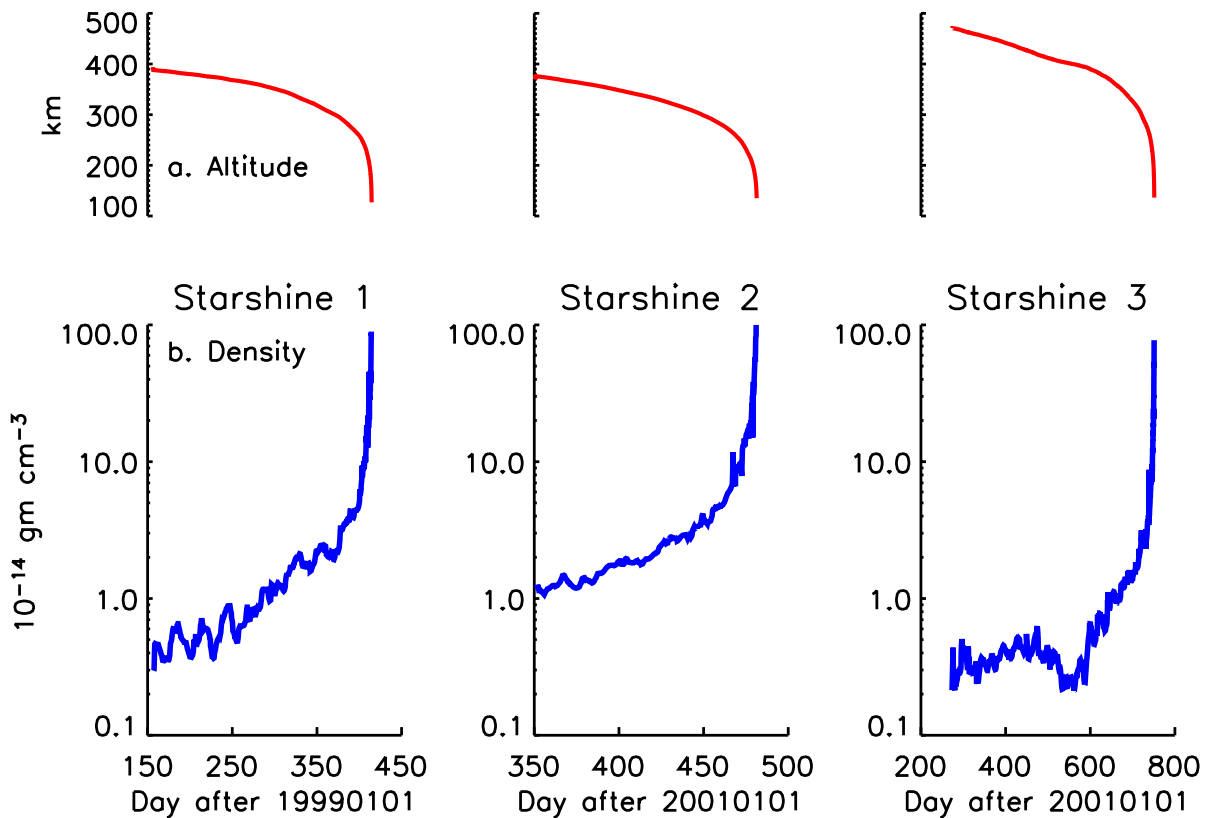


Figure 5. Approximate altitudes of each Starshine spacecraft are shown in the top panel, and compared in the bottom panel are the corresponding mass densities derived from Equation 7 using the quantities in Figure 3 and Table 1.

Figure 6. Altitude profiles of the total mass densities deduced from the drag on the Starshine spacecraft are compared with each other, and with the 1976 US Standard Atmosphere profile.

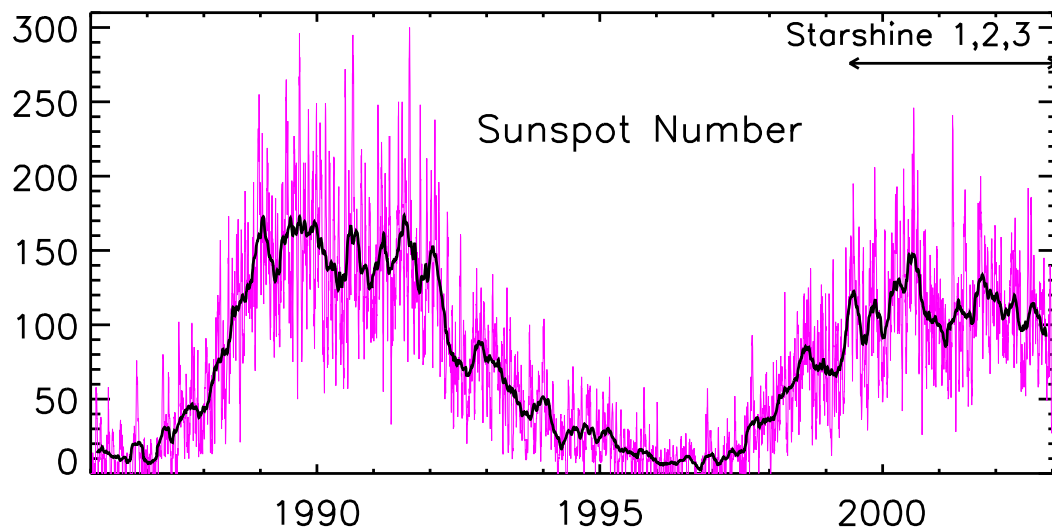
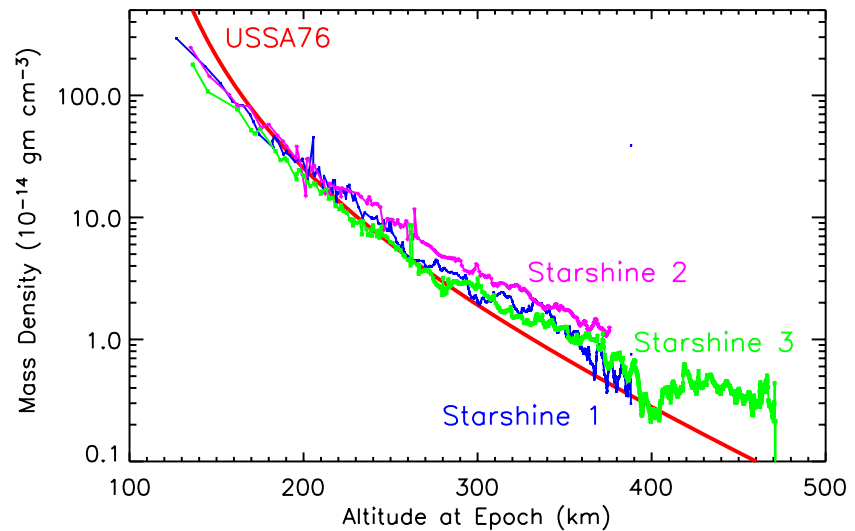


Figure 7. Shown are the daily sunspot numbers in solar activity cycles 22 and 23. The three Starshine missions occurred near the peak of solar cycle 23, which commenced in 1996.

NRLMSIS Upper Atmospheric Density Specifications During the Starshine Missions

The Earth's atmosphere in the region of the lower and middle thermosphere, where the Starshine spacecraft orbits are located, comprises atomic oxygen, O, and molecular oxygen and nitrogen, O₂ and N₂. Figure 8 shows the typical range of upper atmosphere composition variations from the minimum to the maximum of the solar activity cycle. The species, and the total density, vary continuously

throughout the cycle because of variable heating by solar EUV radiation as a result of solar activity.

Given information about solar and geomagnetic activity, the Naval Research Laboratory Mass Spectrometer and Incoherent Scatter (NRLMSIS) upper atmosphere density specification model (*Picone et al., 2000, 2002a*) estimates temperature, total mass density and composition within the original MSIS framework (*Hedin, 1991*) at altitudes up to 1000 km, at any specified geographical location, time and day of year.

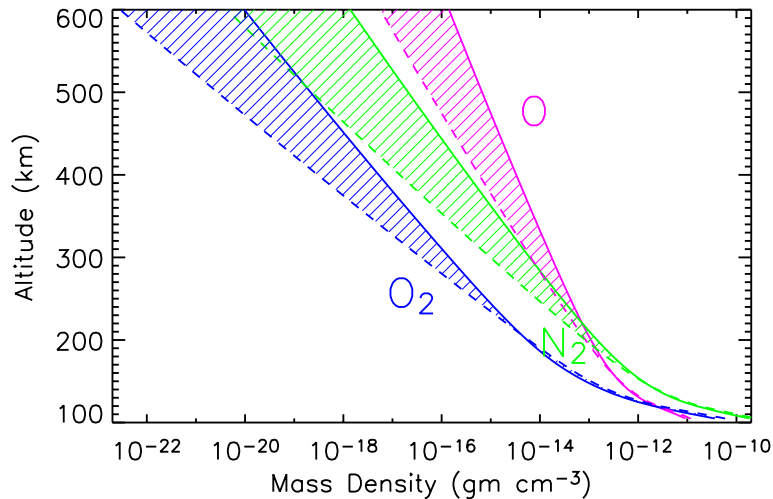


Figure 8. Shown are the mass densities of the primary species of the upper atmosphere at altitudes of the Starshine orbits. The solid lines correspond to high levels of solar activity and the dashed lines correspond to solar minimum conditions.

NRLMSIS utilizes the daily 10.7 cm radio flux, $F_{10.7}$, and its 81-day running mean as a proxy for solar EUV radiation. The A_p index is a proxy for solar-induced perturbations of the Earth's magnetic field. Figure 9 provides daily values of $F_{10.7}$ and A_p for the duration of the Starshine 1, 2 and 3 missions.

The mass densities shown in Figure 5 as functions of time for each Starshine orbit correspond to orbital average values at the TLE epochs. However, the altitudes of the Starshine spacecraft can vary by as much as 30 km during any single orbit (e.g., Figure 4), and the altitudes at each TLE epoch can also vary depending on where in the orbit the TLE was

reported. As well, the latitudes and longitudes of the spacecraft vary throughout the orbit. Comparisons with the drag-derived densities thus require that the NRLMSIS model be evaluated at each altitude, latitude and longitude around a full Starshine orbit at each TLE epoch. Figure 10 shows examples of the altitudes (above the Earth's surface), latitudes and longitudes for individual orbits of each of the three Starshine spacecraft, and the corresponding mass densities calculated by the NRLMSIS model. Orbital averaged NRLMSIS densities at the TLE epochs are compared in Figure 11 with the densities derived from the Starshine spacecraft drag using Equation 7.

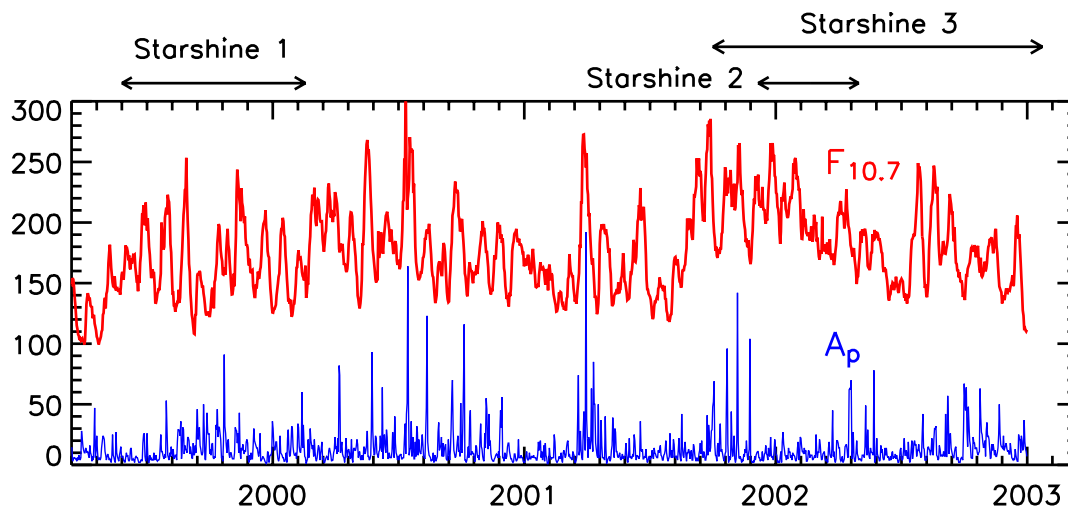


Figure 9. Shown are daily solar radio fluxes, $F_{10.7}$, and daily geomagnetic indices, A_p , during the Starshine missions. The NRLMSIS model uses these proxies to account for the effects of solar and geomagnetic activity on the total mass density of the upper atmosphere.

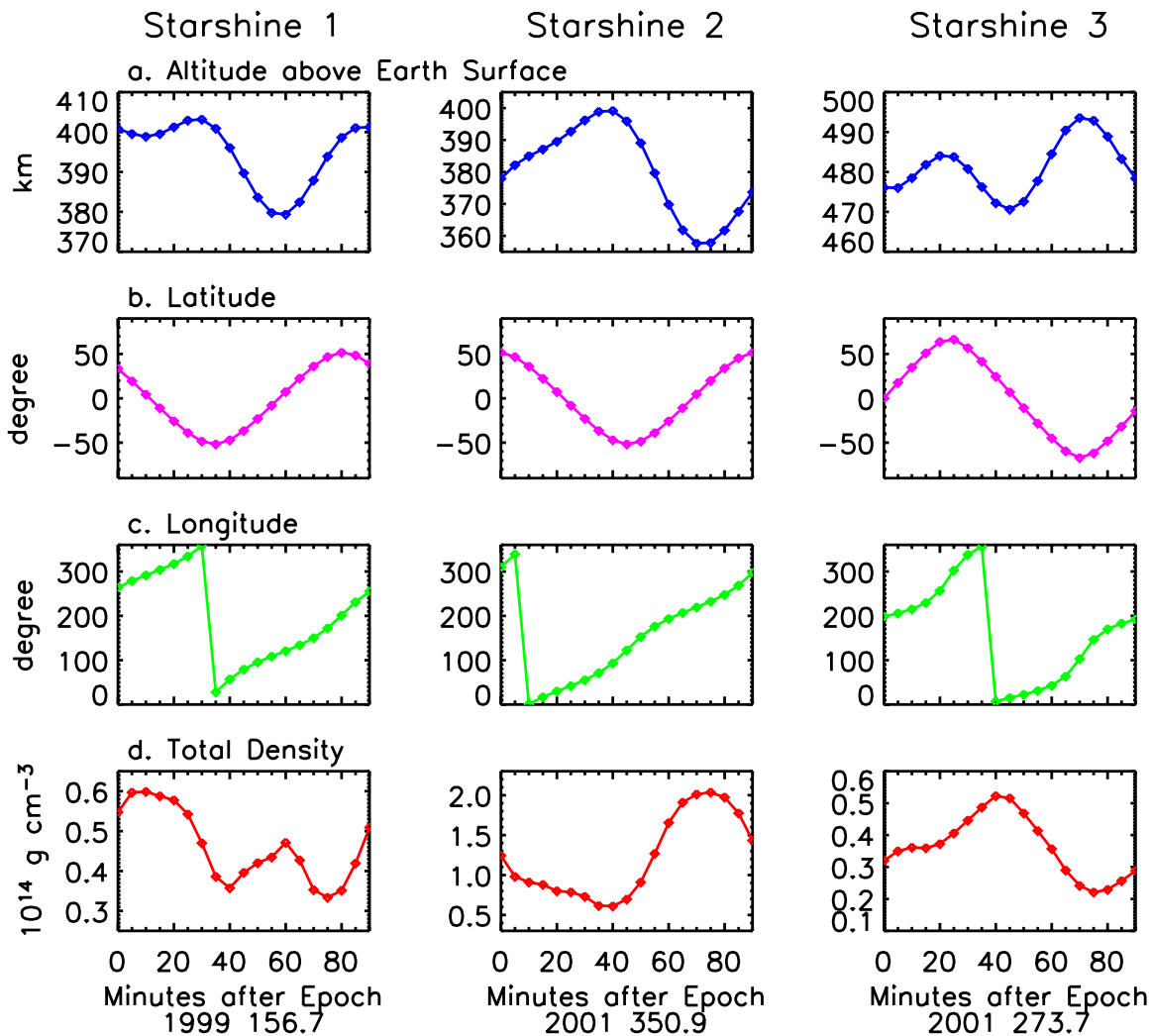


Figure 10. Shown in the four panels from top to bottom are the variations during a single orbit of the altitude, latitude, longitude and mass density for each of the Starshine spacecraft. The NRLMSIS model calculates the mass densities corresponding to the altitude, latitude and longitude.

The comparisons in Figure 11 show that the mass densities derived from Starshine spacecraft typically agree with the densities estimated by the NRLMSIS model to within $\pm 20\%$. The time series of the density ratios in the lower panel of Figure 11 indicate that the differences are not constant in time (nor hence in altitude). As well, the differences between the observed and modeled densities appear to have somewhat regular semi-periodic variations.

Prior results have traced uncertainties in upper atmosphere density specification models to deficiencies in the $F_{10.7}$ proxy that the models use for input. Day-to-day fluctuations in the 10.7 cm radio flux primarily reflect changes in radiation emitted from the corona, the Sun's hot, outer layer. However, the strongest sources of upper atmospheric heating fluctuations, such as the strong 30.4 nm line, are emitted from the cooler and lower chromosphere.

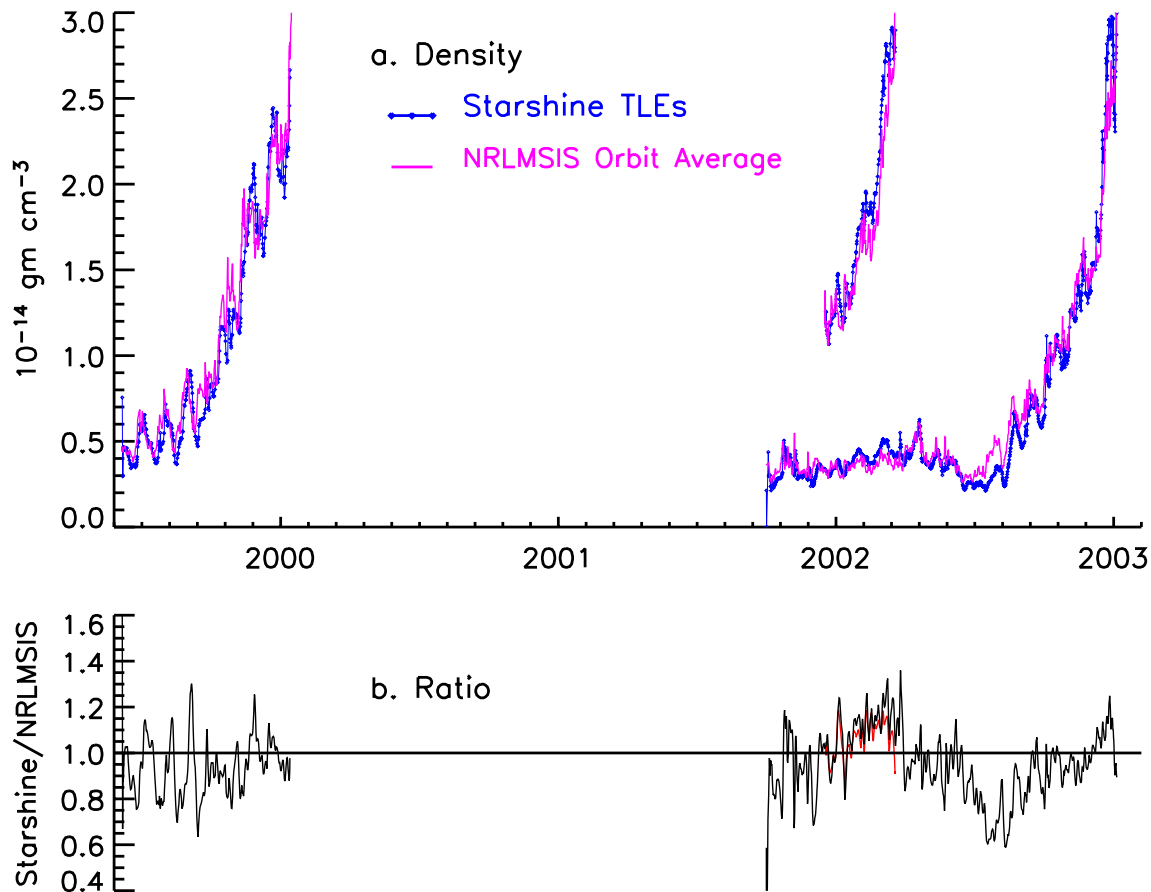


Figure 11. Compared in the upper panel are total mass densities derived from atmospheric drag on the three Starshine spacecraft (shown as symbols) and NRLMSIS densities calculated as the average density along one complete orbital track at the TLE epoch (shown as solid lines). In the lower panel are the ratios of the Starshine and modeled densities.

Our earlier analysis of the differences between the Starshine 1 and NRLMSIS densities (*Picone et al., 2002b*) suggests that these differences track the differences between a chromospheric index of EUV radiation and the $F_{10.7}$ coronal indicator that NRLMSIS inputs as an EUV radiation proxy. While solar chromospheric and coronal indices are similar in that both exhibit marked 11-year cycles, they nevertheless differ in their day-to-day fluctuations. A particular difference is that chromospheric flux rotational modulation is smaller, relative to its solar cycle amplitude than is the case for $F_{10.7}$. As well, the phasing of the 27-day rotational modulation differs for chromospheric and coronal indices, and this appears to contribute to the differences between the upper atmospheric densities derived from Starshine

spacecraft drag and NRLMSIS on time scales of days to months. An improved solar EUV irradiance index may therefore permit the NRLMSIS model to better estimate actual density changes, possibly reducing their uncertainties to below 20%.

The NRLMSIS model is being reformulated using a new chromospheric index to replace $F_{10.7}$. The new model will then be tested with the densities derived from the drag on the Starshine spacecraft. We also plan to use the Starshine orbits to investigate the suitability of the approximate Equation 7 for estimating atmospheric densities of circular orbits at the epoch of each TLE, compared with Equation 5, which requires evaluation of the integral of Fv^3 over the time interval between successive TLE epochs.

Model Validation During Solar Minimum with Additional Starshine Spacecraft

An overall goal of Project Starshine is to educate students about the drag of the upper atmosphere on objects in low-Earth orbits. Thus the program plan calls for a series of spacecraft to extend through the range in solar EUV heating and drag that occurs during the 11-year solar activity cycle. Whereas the first three Starshine spacecraft were launched during times of relatively high solar activity, two additional Starshine spacecraft are planned for launch during solar minimum conditions. The 19"-diameter Starshine 4 satellite, with a 4"-diameter Starshine 5 subsatellite mounted inside it (designed to be released into its own orbit one minute after Starshine 4 is deployed from its launch vehicle) await a Shuttle launch. In this regard, the application to subsequent Starshine missions 4 and 5 of the TLE analysis demonstrated here for Starshines 1, 2 and 3 will provide a unique dataset of upper atmospheric densities for the validation of NRLMSIS models on time scales ranging from days to the solar cycle.

Acknowledgments

NASA's Living with a Star Program and ONR supported this work.

References

- Hedin A., Extension of the MSIS thermospheric model into the middle and lower atmosphere, *J. Geophys. Res.*, 96, 1159-72, 1991.
- King-Hele, D. G., *Satellite Orbits in an Atmosphere: Theory and Applications*, Blackie, Glasgow and London, 1987.
- Picone, J. M., A. E. Hedin, D. P. Drob, J. Lean, A. C. Nicholas, and S. E. Thonnard, Enhanced empirical models of the Thermosphere, *Phys. Chem. Earth* ©, 25, 537-542, 2000.
- Picone, J. M., A. E. Hedin, D. P. Drob, and A. C. Aikin, NRLMSISE-00 Empirical Model of the Atmosphere: Statistical Comparisons and Scientific Issues, *J. Geophys. Res.*, Vol. 107, No. A12, 1468, doi:10.1029/2002JA009430, 24 December 2002a.
- Picone, J. M., J. Lean, S. Knowles, A. Hedin, and G. Moore, "Validating NRLMSIS Using Atmospheric Densities Derived From Spacecraft Drag: Starshine Example", in *Proceedings of 2002 AIAA/AAS Astrodynamics Special Conference*, Monterey, CA American Institute of Aeronautics and Astronautics, 2002b.